



Deposited via The University of Sheffield.

White Rose Research Online URL for this paper:

<https://eprints.whiterose.ac.uk/id/eprint/219067/>

Version: Published Version

Article:

Patel, A.D., Schyns, Z.O.G., Franklin, T.W. et al. (2024) Defining quality by quantifying degradation in the mechanical recycling of polyethylene. *Nature Communications*, 15 (1). 8733. ISSN: 2041-1723

<https://doi.org/10.1038/s41467-024-52856-8>

Reuse

This article is distributed under the terms of the Creative Commons Attribution (CC BY) licence. This licence allows you to distribute, remix, tweak, and build upon the work, even commercially, as long as you credit the authors for the original work. More information and the full terms of the licence here:

<https://creativecommons.org/licenses/>

Takedown

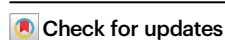
If you consider content in White Rose Research Online to be in breach of UK law, please notify us by emailing eprints@whiterose.ac.uk including the URL of the record and the reason for the withdrawal request.

Defining quality by quantifying degradation in the mechanical recycling of polyethylene

Received: 12 April 2024

Accepted: 24 September 2024

Published online: 09 October 2024

Arpan D. Patel^{1,2}, Zoé O. G. Schyns^{1,2}, Thomas W. Franklin^{1,2} & Michael P. Shaver^{1,2} ✉

Polyolefins have a multitude of uses across packaging, automotive and construction sectors. Their resistance to degradation during reprocessing enables recyclability, but variability in recycled polymer feedstocks renders it difficult to assure their manufacturing suitability. The lack of quality control methods has disabled circular economy pathways; product failure is costly, wasteful and time-intensive. Using rheology-simulated and extrusion-based recycling experiments, we explore the degradation pathways of high-density polyethylene (HDPE). Chain scission dominates during the initial degradation of HDPE, and increasing exposure to O₂ shifts the dominant mechanism to long-chain branching. Importantly, extending this method to post-consumer recycle (PCR), the results show potential as a methodology to assess recycle quality to enable a circular plastics economy. In this study, we establish the validity of this rheology simulation to define a characteristic degradation parameter, relating it to the structural evolution under different environments defined for virgin HDPE and post-consumer recycle (PCR).

Plastics are a globally pervasive material due to their versatility, low cost and robust properties¹. But mismanagement of plastic waste at end-of-life is problematic; over 50% of plastic manufactured is disposed of with no method of recoupment^{2–4}. This linear economy for plastic necessitates continual resource extraction, processing, and energy consumption that could be avoided through recycling plastic feedstocks⁵, potentially saving over 300 MtCO₂e per annum⁶. Despite this environmental benefit, mechanical recycling is languishing. The mechanical, optical, and thermal properties of recycled plastics do not match those of virgin resin and the financial costs of high-quality recycle are prohibitive^{7,8}. Retaining plastic value at end-of-life is essential for a circular plastics economy, but to prevent the adoption of low-value end-of-life strategies (e.g. landfilling, incineration, pollution) we must understand how structure-property relationships within recycled polymers are tied to plastic quality.

Polyolefins account for 32.2% of packaging collected from waste in the UK, [polyethylene (PE): 22.0% and polypropylene (PP): 10.2%]^{3,9}. This class of polymers has a wide range of applications due to their structural simplicity and strong physical properties—ranging

from food containers, rope, and fibres to roofing materials and facemasks^{10–12}. During the mechanical recycling process, polymers are subjected to heat and high shear forces (up to 10⁵ s⁻¹)¹³ which causes thermo-oxidative and thermo-mechanical degradation. Chain-scission or chain-extension reactions spark from shear or temperature-induced β-chain scission. The primary free radicals formed can recombine, react with O₂, or form secondary radicals via hydrogen abstraction. Long-chain branching (LCB), multiple oxidation products that promote further degradation (e.g. carboxylic acids, ketones, aldehydes or lactones) and subsequent intramolecular radical transfer^{3,11,14,15} all complicate processing due to changes in melt-flow rate, and thus limit recycle quality by reducing mechanical performance relative to virgin feedstocks¹⁶. Despite these challenges, polyolefins are some of the most recycled materials, with pristine feedstocks withstanding multiple rounds of high-temperature processing because of their stable homo-atom backbones¹⁷.

The compositional variability in real-world recycle^{18,19} leads to highly variable feedstocks in molecular weight, intentionally and non-

¹Department of Materials, School of Natural Sciences, University of Manchester, Manchester, United Kingdom. ²Sustainable Materials Innovation Hub, Henry Royce Institute, University of Manchester, Manchester, United Kingdom. ✉e-mail: michael.shaver@manchester.ac.uk

intentionally added substances and polymer contaminants. Degradation is specific to polymer grade, process parameters and equipment and thus is unpredictable^{20,21}. This grade-specificity and compositional-specificity necessitates expensive segregation of higher quality feedstocks and additional additives exacerbating the economic barriers to circularity^{22,23}.

The extrusion environment plays an important role in dictating the degradation mechanisms of polyolefins²⁴. Macroradicals reacting in oxygen-rich environments result in stable carbonyl and hydroxyl end groups, producing a synergistic effect where end groups act as radical acceptors, subsequently reacting with each other leading to LCB formation^{15,25}. However, in inert atmospheres, chains are protected from oxygen- or hydroxyl-based radicals and chain scission dominates from shear-induced degradation²⁶. Temperature has been cited as the most important factor contributing to high-density PE (HDPE) degradation, but little work has been completed on investigating the effects of different gas environments on HDPE degradation²⁷. However, all of these extrusion-based studies are laborious, expensive, and time-intensive. It is challenging to relate this fundamental understanding to the compositional variability observed in recycle; this makes the incorporation of recycled content into plastic products either risky, expensive or both.

We hypothesized that rheology would be a powerful tool to determine feedstock properties and measure recycle quality (Fig. 1). The quality of plastic feedstocks has been previously estimated by the level of contamination²⁸. Contaminants include material impurities (e.g. cardboard, dyes, foodstuffs) with their presence accelerating degradation²⁹. Contamination by other resin codes (e.g. PP in a PE waste stream) forms immiscible blends with diminished properties due to the incompatibility of polymer phases. However, as additive and contamination levels are not known, plastic producers remain unable to use recycle efficiently.

In this study, we assess the limits to polyolefin degradation by developing a rheological method to simulate extrusion conditions. This facile method mimics the mechanical recycling of a polyolefin while reducing the need for time and resource-intensive extrusion experiments³⁰. Providing a measure of feedstock degradation before a manufacturing process can inform whether it is suitable for end-consumer use and minimise the need for expensive additives. Application and automation of this methodology are possible with in-line rheological measurements via decision trees—suitable for the production of smart factories and industry 4.0³¹. By initially validating the method on virgin and post-industrial recycle streams, we then extend the methodology to assess different commercial sources of post-consumer recycle (PCR), showing it to be a powerful tool to assess the propensity to degradation – or recycle quality – for polyethylene.

Results and discussion

Pristine polyolefins display minimal structural changes with repeated extrusions; HDPE can be reprocessed up to 100 times before significant degradation¹⁷, in contrast to real-world recycling efforts where composition and contamination change thermo-mechanical and thermo-oxidative degradation pathways³². To validate the applicability of simulated recycling methodology to mechanical recycling, a single grade of virgin HDPE was mechanically recycled 5 times and characterised to create a baseline reference for rheological analysis (Fig. S1A).

Polyolefin degradation mechanisms in simulated recycling

The mechanical recycling process was simulated using a bespoke rheological experimental design. Consecutive frequency sweeps were performed over 3 hours in controlled gaseous environments (air and N₂) to investigate the changes in the structure of polyolefins (Figs. 2, 3).

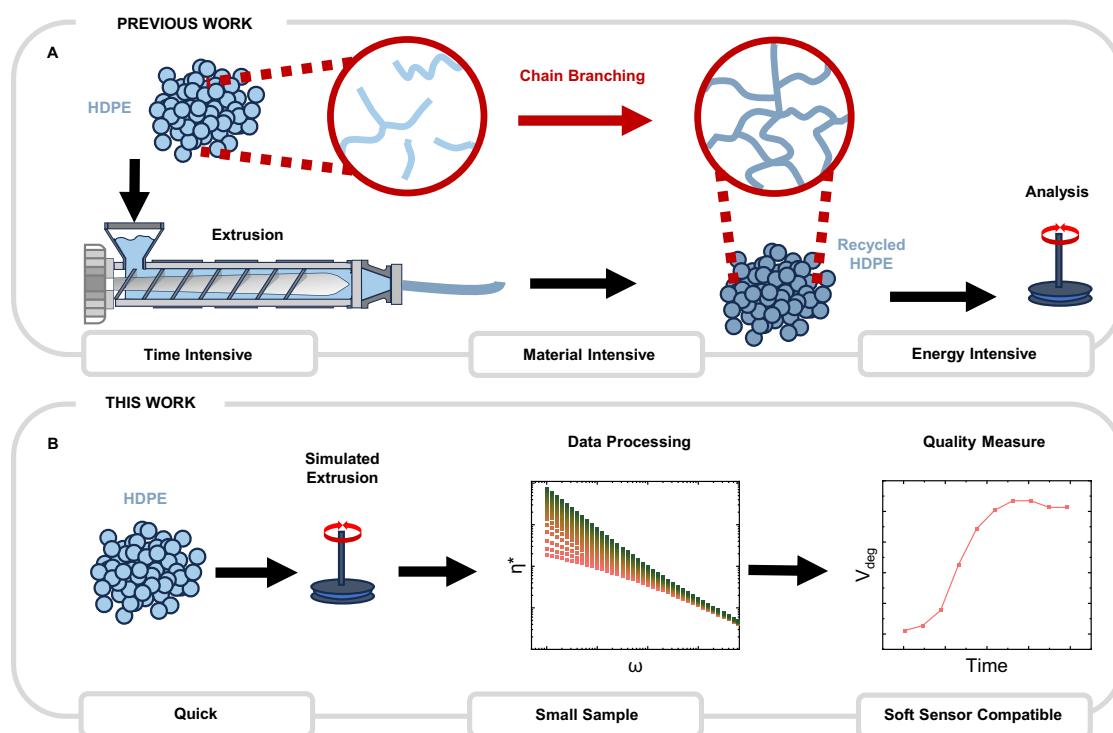


Fig. 1 | Overview of existing mechanical recycling analysis versus simulated work as reported in this paper. **A** Previous work entails processing HDPE via extrusion, leading to thermo-mechanical and thermo-oxidative degradation under heat and shear. This leads to degradation within polymer chains leading to long-

chain branching. **B** In this work, we aim to reduce the time required to analyse the mechanical recycling process by simulating it using melt rheology in a fraction of the time. Data is then extracted, processed, and transformed to provide an indicator for polymer degradation—the extent of long-chain branching within HDPE.

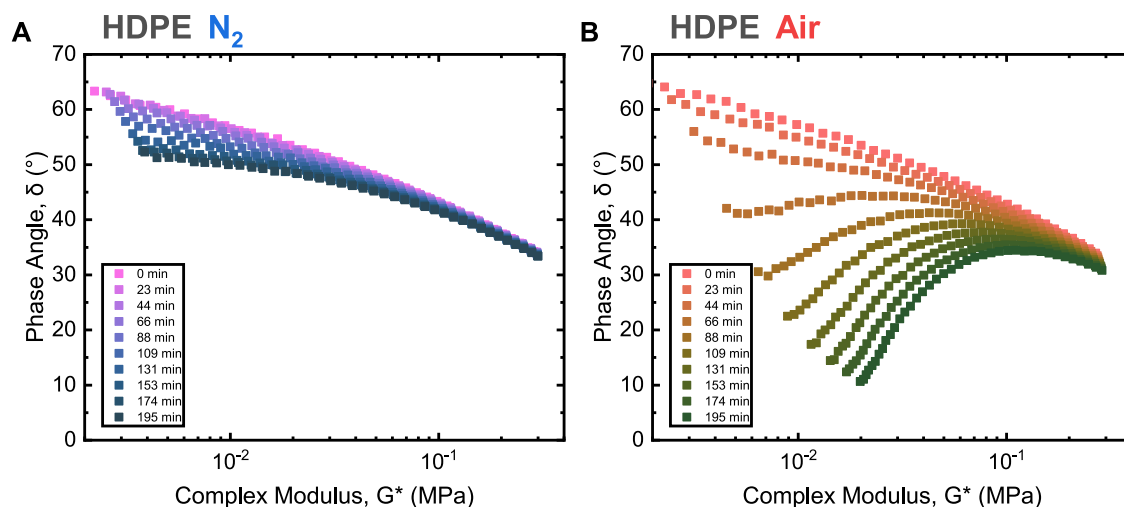


Fig. 2 | Rheological recycling simulation of HDPE. Van Gorp-Palmen plot of rheological recycling simulation in N_2 (A) and air (B) as determined from successive frequency sweeps (Figs. S3, S4). A Van Gorp Palmen plot is a measure of complex modulus, in this case, the resistance of HDPE to deformation, and phase angle highlighting the phase behaviour of the polymer melt. Rheological recycling simulations are performed under continuous heat and shear, inducing thermo-mechanical and thermo-oxidative degradation on the polymer melt. This is measured periodically, with the shape of the plot outlining the extent of chain

branching, the primary mechanism of degradation within HDPE. The greater the incidence of the curve within a Van Gorp-Palmen plot, the greater the chain branching measured. Here we see within Air (B) there is a measurable increase in the amount and rate of chain branching within HDPE as compared to using an inert environment, N_2 (A). This is shown in the plot with a decreasing phase angle, indicating more solid-like behaviour and greater resistance to deformation, resulting from greater chain branching.

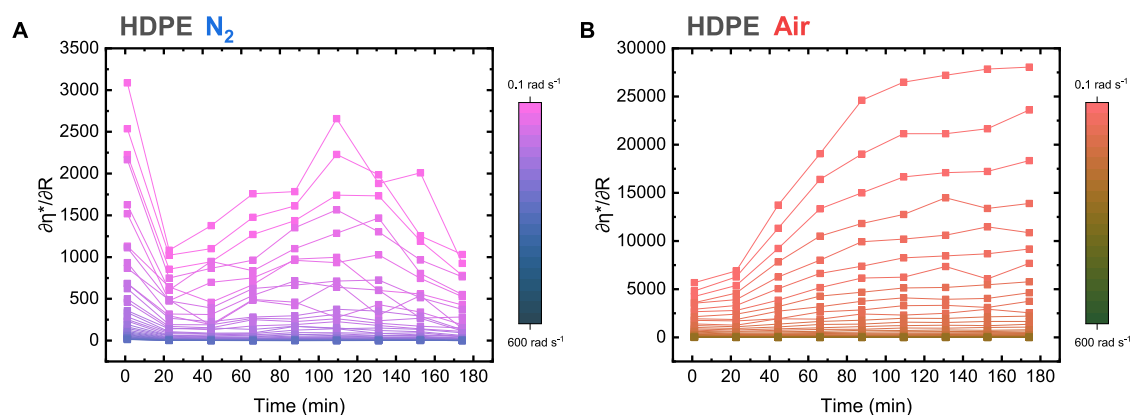


Fig. 3 | Change in complex viscosity during rheological recycling simulation of HDPE. Rate of change of complex viscosity during rheological recycling simulation in N_2 (A) and Air (B) as determined from complex viscosity at different angular frequencies during sequential frequency sweeps at 200 °C, from 0.1 to 600 rad s^{-1}

at 0.3 % strain (Figs. S3, S4). Of note is the order of magnitude difference between the rate of change of complex viscosity with time, derived from the increasing amount of long-chain branching with simulations under air.

Oscillatory shear applied at extrusion temperatures was found to mimic the conditions of mechanical recycling via high-temperature twin-screw extrusion as evidenced by similar viscoelastic responses from the material with oscillatory testing and similar zero shear viscosity profiles (Fig. S1). These rheological conditions were hypothesised to induce chain scission of the polymer via radical-induced hydrogen abstraction. Importantly, the mechanism of radical attack changed according to the gaseous environment. Limiting the presence of O_2 within the reaction environment minimised thermo-oxidative degradation and thus the extent of chain scission (Fig. 2), corroborating previous results³³.

Our initial measurements confirmed a change in the complex viscosity (η^*) and the cross-over modulus of molten HDPE; rheological behaviour being a strong indicator of changes in molecular structure (Fig. S2)³⁴. In N_2 , the complex viscosity of HDPE increased by 14% at an angular frequency of 10 rad s^{-1} (Fig. S3A)—which is the angular frequency approximately equivalent to the rotation of an extruder at

100 rpm—post-simulated recycling treatment. The changes in the rubbery plateau region, indicated by modulus crossover, are used to estimate changes in molecular weight and polydispersity for polyolefins^{34,35}. From the modulus crossover, we see an increase in weight-average molecular weight (M_w) and a broadening of the molecular weight distribution (MWD) corresponding to a chain branching degradation mechanism (Fig. S2A)^{35,14,36,37}. In air, $G' > G''$, suggests that the behaviour is more solid-like (i.e. elastic > viscous) and indicates that branching within the sample is significant (Fig. S2B)^{30,38,39}.

The Van Gorp-Palmen (vGP) plot is a refined method to qualitatively study the thermo-rheological complexity of polymeric materials, by directly measuring phase angle, δ , as a function of the magnitude of the complex modulus, $|G^*|$. The phase angle and complex modulus are functions of the angular frequency, ω , (Eq. S3) and, with time-temperature superposition principle validity, is independent of both frequency and temperature⁴⁰. The time-temperature superposition

principle holds true for linear pristine polymers, with highly branched systems failing to superpose within a vGP plot (Fig. S23).

The vGP plot can be used to elucidate basic characteristics for simple linear polymers—normally a curve characterised by a minimum and an inflection point. An increasing complex modulus is indicative of improved resistance to deformation, whereas changes in phase angle suggest increasing elastic (solid-like) or viscous (liquid-like) behaviour. The shape of the curve is strongly correlated to the crossover modulus, molecular weight, and dispersity of a polymer. These changes in curvature correspond to new relaxation mechanisms of polymer branches^{41,42}. The initial vGP shape of HDPE treated in N₂ supports the presumptive chain scission mechanism: a flattened curve with a consistent phase angle, indicating that no additional relaxation modes arise through formation of branches. With time, however, a gradual increase in complex viscosity and vGP curvature suggests a shift towards a long-chain branching mechanism (Fig. 2A). Chain scission results in shorter polymer chains that are less prone to further scission³³ as they reach a maximum stable chain size; however, these shorter fragments are still susceptible to attack from longer chain macroradicals which may result in branching.

Upon changing to test environment to air, the change in complex viscosity (at $\omega = 0.1 \text{ rad s}^{-1}$) post-treatment is 5 times higher relative to samples treated in N₂ (Fig. S4A). Increasing curvature in the vGP plot with successive frequency sweeps, resulting in the phase angle at 0.1 rad s^{-1} tending to lower values (Fig. 2B), suggests that LCB dominates. We hypothesise that the presence of O₂ molecules during treatment leads to LCB through the formation of linkages between new carbonyl end groups along the polymer backbone. Carbonyls may act as intermolecular radical acceptors²⁵, promoting macroradical attack and causing LCB.

The rate of change in viscosity relative to frequency sweep ($\frac{\partial \eta'}{\partial \omega}$) repetition can be extracted from rheological experiments and is thus indicative of the evolution of the HDPE structure. In samples treated in N₂, viscosities are slightly upshifted during testing (Fig. S3C), with the rate of change of viscosity post initial frequency sweep ($t = 22 \text{ min}$) increasing to a secondary peak (6th frequency sweep, $t = 109 \text{ min}$) and subsequently decreasing until the end of the experiment (Fig. 3A). This contrasts with HDPE samples treated in air, during which a constant increase in complex viscosity was observed (Fig. S4C), corresponding to an accelerated rate of change with each consecutive sweep (Fig. 3B). These trends in data are mirrored across vGP plots, in which distinct mechanisms are observed between air and N₂. The structural changes observed during these rheological tests of polyolefins correspond with mechanical recycling degradation mechanisms presented in literature^{3,17,26,29,33,36,43}, validating the hypothesis that this modified rheological method can be used to assess the propensity for degradation. Further discussion can be found in Section 3 of the supporting information.

Classifying polyolefin degradation via Van Gorp-Palmen plots

Characterizing polyolefin degradation mechanisms is challenging. Within the terminal regime, i.e. at low angular frequencies, the imaginary (G'') and real (G') components of the complex modulus are closely related (Eq. S4). The linear steady-state recoverable compliance, J_e^0 , plays an essential role in molecular analysis, as it characterizes the elasticity of a polymer (Eqs. S5, S6). This recoverable compliance is directly related to its retardation spectrum, the fingerprint of molecular motions^{39,40}. Zero shear viscosity, η_0 , also plays an important role in the structural analysis of polymeric materials as it is directly proportional to critical molar mass—a relationship well documented for linear PE (Eqs. S7, S8)^{39,44–46}. A small change in molar mass can have a large impact on η_0 , and thus is a sensitive tool to probe polymeric thermal stability.

The relationship between η_0 and G^* provides practical validity for the use of rheology to probe the degradation of linear PE indirectly as

this relationship fails for increasingly branched species^{39,40}. High molar mass components can significantly impact polyolefin elasticity within the linear range of deformation but are difficult to measure via high-temperature size exclusion chromatography (HT-SEC)³⁹. HT-SEC alone is unsuitable for quantitatively probing PE quality. The effect of long-chain branches on elasticity is also pronounced but difficult to quantify. Reducing the interactions of polymer chains of varying lengths to a quantitative measure is difficult, due to the mathematical complexity involved in this process and the size of polymer chains. However, changing J_e^0 can be an indicator of changes in molar mass, with deformation of linear polymers that have undergone LCB, having a higher recoverable compliance⁴⁰. While long-chain branches increase the elasticity of PE, the type of branching that it undergoes during degradation remains difficult to discern.

For these reasons, the vGP plots serve as an important tool in quantifying changes in PE structure during degradation, with an increasing branching structure leading to an increase in elasticity, which changes the curvature of the plot. While a specific branching mechanism is difficult to ascertain from a single measurement, the degree of branching within a sample can be estimated over a simulated recycling study, directly relating observed changes to thermo-mechanical and thermo-oxidative degradation mechanisms³.

Taking Fig. S7 as an example, as the change in the gradient of the terminal regime (ω ranging from 0.31 to 3.16 rad s^{-1}) in the vGP plot becomes shallower with time, the elasticity of the polymer increases, suggesting an increase in chain branching and dispersity of PE. This change in elasticity, indicated by a terminal flow plateau, demonstrates viscous behaviour at lower complex moduli⁴². The degree of chain branching is qualitatively linked to the availability of O₂ and thus the propensity for thermo-oxidative over thermo-mechanical degradation.

This complex framing of the data can be reduced to a 'degradation value' calculated based on the curvature of the vGP plot; comparing polymer that has not been processed (virgin material) to extensively treated material and producing upper and lower limits of polymer 'quality'. The gradient along the terminal regime of the vGP plot can be described as follows:

$$V_{deg} = \lim_{0.31 \leq \omega \leq 3.16} \frac{\partial \delta}{\partial |G^*|} \quad (1)$$

Where:

V_{deg} is the change in gradient along the vGP plot when ω , the measured angular frequency is between 0.31 and 3.16 rad s^{-1} .

$\partial \delta$ is the change in phase angle.

$\partial |G^*|$ is the change in complex modulus.

Equation 1 provides a characteristic quantitative value, V_{deg} , which is proportional to the degree of degradation a specific polymer has undergone through mechanical processing.

The limits to angular frequency (0.31 – 3.16 rad s^{-1}) are chosen to represent the area of the terminal regime where the relationship between zero shear viscosity, η_0 , angular frequency, ω and the linear recoverable steady state compliance, J_e^0 (outlined in Eqs. S5 and S6) holds. This choice of limits maximises the degree of change in the long-range structure of the polymer, indicative of thermo-oxidative degradation.

This classification is polymer-dependent but can be made independent once the complex modulus, G^* , is reduced by dividing the complex modulus values by the complex modulus minima along the vGP curve. Using this reduction features such as chemical composition, tacticity and monomer composition in copolymers no longer influence the curve⁴². This value will measure the extent of chain branching relative to pristine linear polymers. While chain scission plays an important role in polymer degradation, especially in other packaging polymers³⁰, and will be challenging to observe with this

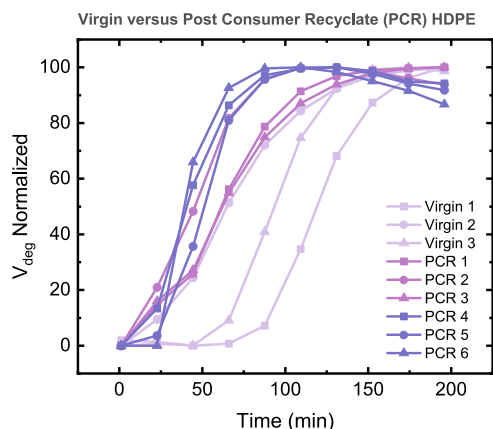


Fig. 4 | Plot of V_{deg} versus time for multiple virgin grade HDPEs when compared to Post Consumer Recyclate (PCR) HDPE under air during rheological simulated recycling. Virgin 1–3 are commercial HDPEs, used in bottle manufacturing. PCRs 1–3 are commercially available 'Natural' grade feedstocks. PCRs 4–6 are 'Jazz' grade feedstocks. Normalised to [0,100]. Measurements taken at 200 °C, from 0.1 to 600 $\text{rad}\cdot\text{s}^{-1}$ at 0.3% strain with 12-minute intervals. V_{deg} allows for a comparative measure of the rate of degradation of multiple grades of HDPE and can be key to determining polymer feedstock quality.

methodology at lower levels of processing, the extent of chain branching is the predominant factor in both PE degradation and mixed waste (PE/PP blends).

We can thus define a V_{deg} minimum, as V_{deg} after one sweep under N_2 , and maximum, as the V_{deg} of a fully LCB system after extended treatment in air, (Fig. S9) and compare how a polymer degrades under extrusion with time (Fig. S10). The change in V_{deg} provides a kinetic estimation of degradation with time. Under treatment in an N_2 environment, the rate of change of V_{deg} of HDPE remains constant, indicating that the shift towards LCB is consistent through time. Conversely, under an O_2 -containing gas flow, the rate of change of V_{deg} increases significantly, resulting in a degradation mechanism that rapidly shifts towards a pure LCB.

Assessing quality of post-consumer recyclate

The power of the methodology developed is shown when applied to a range of virgin grades of HDPE as well as commercially sourced PCR, as shown in Fig. 4. Further specification of these PCRs is available in the supporting information. Previous analysis has shown that categorisation of PCRs using chemometric techniques such as principal component analysis and decomposing the vibrational data of polymers is complex¹⁸. With low confidence intervals when sampling is not sufficient, it is difficult to delineate different grades of the same polymers from each other. The variability of composition in industrial-scale mechanical recycling necessitates the development of methods; the application of V_{deg} to a range of HDPEs with differing qualities can validate the methodology in assessing mechanical recycling.

From our analysis, the V_{deg} of most grades of PCR is higher than that of virgin HDPE in the early stages of the recycling simulation (Figs. 4, S18). During further processing, the rate of degradation for vHDPE overtakes that of PCR, reaching a plateau of V_{deg} at $t = 66$ min. PCR will degrade faster, but also reach its natural degradation limit more easily, while virgin HDPE, composed of predominantly linear chains, would have a greater maximum extent of chain branch. This difference necessitates normalising data (see discussion in Supporting Information), allowing for visualisation of this difference in Fig. 4 through the shallower gradients of V_{deg} in vHDPE *vs.* PCR.

The other key quality metric is a translation of V_{deg} across the time axis (c. 44 min from HDPE to PCR). The extent to which different HDPEs chain branches differ, with grades of virgin HDPE (Virgin 1, 2, 3)

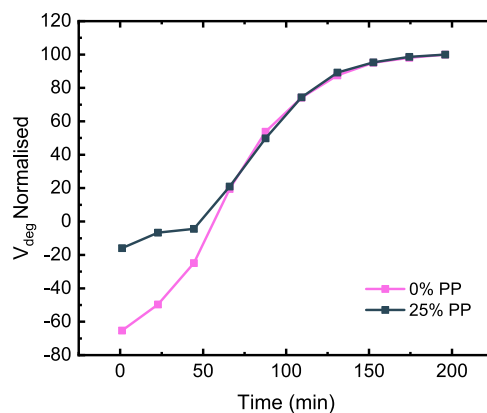


Fig. 5 | Comparison of degradation in HDPE and PP-contaminated HDPE. Plot of V_{deg} versus time for HDPE blends containing 0% PP and 25% PP under air during rheological simulated recycling. Measurements taken at 200 °C, from 0.1 to 600 $\text{rad}\cdot\text{s}^{-1}$ at 0.3 % strain with 12 min intervals with data normalised to maxima for scale.

and 'Natural' grade PCR 1, 2, 3) taking a longer time to chain branch *vs.* lower quality 'Jazz' grade HDPEs (PCR 4, 5, 6) (Figs. S15–S18). This suggests that the stabilising zone of thermo-oxidative degradation is reached sooner for lower-quality PCR, with the rate of chain branching being more significant in lower-quality HDPE. This corroborates with previous analyses, with high and low-quality PCRs matching groups identified via principal component analysis¹⁸. Further feedstock-specific results are discussed in section 10 of the supplementary information.

So-called 'jazz grade' PCRs do not match the mechanical performance of either natural or virgin grade HDPE^{47–51}. Insufficient sorting leads to PP contamination, causing both phase separation and an increase in the amount of long-chain branching^{48,49}. The resultant disruption in epitaxial crystallization all leads to weakened intramolecular bonding within the polymer phase^{50,51}. The result of PP contamination in PE is a low-quality polymer blend, with poorer mechanical properties *vs.* the distinct single resins. To test whether V_{deg} can quantify these impacts we prepared a blend of 25% virgin PP in virgin HDPE and examined its resistance to degradation. Figure 5 shows the V_{deg} values for this PE/PP blend, derived from vGP plots (Fig. S20), with PP chains inducing a much higher propensity for chain branching at early time points before converging with virgin HDPE samples in normalised spectra. This convergence suggests that the total amount of potential chain branching may remain the same between samples but the kinetic profile of this degradation is impacted by PP. Future work will explore the impact of variable %PP contamination in HDPE to test if V_{deg} allows for a comparative measure of degradation rates correlating to PP loadings as a determining factor in polymer feedstock quality. Similarly, this methodology can be used to assess the impact of additives such as stabilising systems. We prepared a challenge sample by coextrusion of the commercial phenolic antioxidant Irganox 1010 at 1% with virgin HDPE, the highest recommended loading to exacerbate a response to thermo-oxidative degradation. The sample, as shown in Fig. S21, showed a dramatic improvement in V_{deg} , suggesting that this method may in the future be used to optimise additive formulations.

The vGP methodology thus can serve as a tool to analytically measure quality. If optionally paired with other characterisation techniques, this technique has the potential to be easily applicable to industry as extruded samples can be rapidly assessed. Quality testing is a key step in the utilisation of recyclate in mechanical recycling where the cost of highly performing PCR exceeds that of vHDPE. This methodology can enable manufacturers to discern highly performing jazz-grade PCR from feedstocks and utilise them in formulations at a

cheaper cost than buying natural-grade PCRs. The future development of rheological soft sensors in mechanical processing could allow for an in-line methodology to gauge plastic quality and contamination then tuned by additive composition. The methodology provides a specific measure of polymer degradation vs. its unprocessed counterpart. This ability to gauge branching through rheological measurements allows for rapid screening of feedstock and correlation to performance. Our future efforts seek to translate this to industry 4.0 manufacturing efforts. In supervised learning models based on classification, such as decision trees, a particular recycled feedstock can be deemed suitable for use if it meets a defined V_{deg} criteria.

Mechanical recycling is the lowest carbon footprint method to enable a plastics circular economy, but feedstock variability prevents wide-scale adoption due to economic and product failure risks from inconsistent composition. An analytical tool to assess the quality of recyclate is urgently needed. We demonstrated that polyolefin degradation can be assessed using rheological recycling simulations, across both thermo-mechanical and thermo-oxidative degradation mechanisms. Competing degradation mechanisms (i.e. chain scission and LCB) can be favoured by switching gaseous environments during high-temperature processing. The resulting changes in molecular structure were quantified by observing increases in complex viscosity after repeated processing and confirmed using Van Gurp-Palmen analysis. A degradation limit was found for HDPE in inert atmospheres (N_2 , CO_2 , Argon); thermo-oxidative degradation can be much more significant, showing the potential importance of a working atmosphere in plastics processing.

We defined a characteristic parameter of degradation, V_{deg} , which can be extracted from vGP data from oscillatory rheological measurements. Calculation of this parameter offers a facile approach to quantify the quality of a polymer feedstock and its tendency to degrade during mechanical recycling. The applicability of V_{deg} to extrusion is a promising technique to determine the extent to which HDPE degrades and a powerful tool to rapidly screen polymer feedstocks; recycling studies at the product level would take weeks of time and kilograms of material. We show that multiple, diverse grades of PCR can be rapidly characterised and their quality-tested relative to different grades of virgin feedstock. In combination with mechanical testing data, this would provide a robust tool to determine the quality and utility of these recycled resins, enabling a circular economy.

Methods

Materials

For recycling simulations two virgin polyolefins were used; food grade HDPE (Sabic® HDPE B624LS, MFR: $0.5 \text{ dg}\cdot\text{min}^{-1}$ at 190°C and 2.16 kg , ρ : 0.962 g cm^{-3} , melting point (mp) = 135°C) was purchased from Hardie Polymers and food grade PP (Total Energies PPH 10042, MFR: $35 \text{ dg}\cdot\text{min}^{-1}$ at 230°C and 2.16 kg , ρ : 0.905 g cm^{-3} , mp = 165°C) was purchased from Plasticserv. Gases (N_2 , Air) were supplied by BOC cylinders (N5.0). Mixed O_2 : N_2 gas AZ-size cylinders with purities of (N2.6 O_2 , N4.8 N_2 , mixtures of 5%, 10%, 16%, and 21% O_2 content) were supplied by BOC specialty products.

For the comparative PCR analysis, three virgin HDPEs of extrusion blow moulding grade were included in this study. These HDPEs are LyondellBasell's Hostalen 5231 D, MFR: $0.2 \text{ dg}\cdot\text{min}^{-1}$ at 190°C and 2.16 kg , ρ : 0.954 g cm^{-3} , mp = 127°C (V1), Sabic® HDPE B624LS, MFR: $0.5 \text{ dg}\cdot\text{min}^{-1}$ at 190°C and 2.16 kg , ρ : 0.962 g cm^{-3} , mp = 135°C (V2), and LyondellBasell's Hostalen 5831D, MFR: $0.3 \text{ dg}\cdot\text{min}^{-1}$ at 190°C and 2.16 kg , ρ : 0.958 g cm^{-3} , mp = 132°C (V3). HDPE PCR samples were selected for inclusion in this analysis on the basis that they were commercially available and listed as extrusion blow moulding grade. These materials were used as received and were compositionally unspecified, thus representative of real-world recyclate. The melt flow rates (MFR) of the PCRs obtained for this study were in the range of 0.1 – $0.89 \text{ g}/10 \text{ min}$ ($190^\circ\text{C}/2.16 \text{ kg}$) and therefore suitable for extrusion

blow moulding. Once received, the PCR pellets were stored in sealed containers under ambient conditions. The PCR pellets' countries of origin included: The United States of America, Netherlands, Italy, Spain, Poland and the United Kingdom.

Rheology

Rheological measurements were performed on a Discovery Hybrid Rheometer-2 (TA instruments) with an environmental test chamber (ETC) using a stainless-steel parallel plate ($d = 25 \text{ mm}$, sample gap = 1 mm). Gas was supplied via ETC flow control at a rate of $15 \text{ L}\cdot\text{min}^{-1}$. Gas mixtures were supplied via individual flow controllers connected to a Push Fit Y-Connector. A mixing section was placed between the supply and flow controllers through extended tubing. Oscillatory amplitude sweeps ($10 \text{ rad}\cdot\text{s}^{-1}$, 0.1 – 100% strain, 200°C) were performed to ensure that the testing strain fell within the viscoelastic region of the polymer melt (0.3% HDPE, 1.0% PP). There was minimal change found in data between extremes of the linear viscoelastic region, equivalent to degree of variance found in testing at a fixed strain (Fig. S22).

Frequency sweeps

Sweeps were performed at 200°C from 0.1-rad s^{-1} to 600-rad s^{-1} under polymer-specific testing strain (0.3% HDPE, 1.0% PP), collecting at 10 points per decade. Measurements were performed in triplicate.

Time sweeps

Time sweeps were performed at 200°C at a frequency of $10 \text{ rad}\cdot\text{s}^{-1}$ and under polymer-specific testing strain (0.3% HDPE, 1.0% PP) for 3 h. Sampling was performed at 60-time points across 3 h. Measurements were performed in triplicate.

Simulated recycling frequency sweeps

Periodic frequency sweeps were collected. Frequency sweeps (200°C from 0.1-rad s^{-1} to 600-rad s^{-1} angular frequency at polymer-specific strain) were performed on the polymer melt with a 12-minute isothermal hold (no oscillation) at 200°C between measurements. This process was repeated 10 times to obtain 10 frequency sweeps. Extended testing was performed obtaining 20 frequency sweeps to determine degradation limits. The rate of change of complex viscosity was calculated using the partial derivative of the complex viscosity relative to the change in run $\left(\frac{\partial \eta^*}{\partial R}\right)$.

Mechanical recycling via twin-screw extrusion

Polymers were sequentially extruded in a twin-screw extruder (HAAKE PolyLab configured with a Rheomex PTW 16/25 OS) at 200°C and 100 rpm screw speed at a fixed polymer feed rate of $1 \text{ kg}\cdot\text{h}^{-1}$. The extrudate was cooled in a temperature-controlled water bath (15°C), dried using an air jet, and then pelletised (HAAKE process 16 varicut pelletiser, 1 mm , speed 2.5). Extrudate was dried for 3 h at 60°C (Fis-treem vacuum oven fitted with Edwards RV5 vacuum pump) and then reprocessed under the same conditions outlined above. This process was repeated 5 times for each polymer. The feed rate of specific polymer pre-extrusion was determined via feeder calibration.

Data availability

All data generated and analysed during this study are included in this published article and its supplementary information. All data generated in this study are provided in the source data file provided with this paper. All data are available from the corresponding author upon request Source data are provided with this paper.

References

1. Thompson, R. C., Moore, C. J., Vom Saal, F. S. & Swan, S. H. Plastics, the environment and human health: current consensus and future trends. *Philos. Trans. R. Soc. Lond. B, Biol. Sci.* **364**, 2153–2166 (2009).

2. Linder, M. Ripe for disruption: reimagining the role of green chemistry in a circular economy. *Green. Chem. Lett. Rev.* **10**, 428–435 (2017).
3. Schyns, Z. O. & Shaver, M. P. Mechanical recycling of packaging plastics: a review. *Macromol. Rapid Commun.* **42**, 2000415 (2021).
4. WRAP. *PlasticFlow 2025—Plastic packaging flow data report, 2018*, <https://wrap.org.uk/resources/report/plasticflow-2025-plastic-packaging-flow-data-report> (2018).
5. Department for Environment Food & Rural Affairs. *Our Waste, Our Resources: A Strategy for England. Department for Environment, Food & Rural Affairs, 2018*, https://assets.publishing.service.gov.uk/government/uploads/system/uploads/attachment_data/file/765914/resources-waste-strategy-dec-2018.pdf (2018).
6. Zheng, J. & Suh, S. Strategies to reduce the global carbon footprint of plastics. *Nat. Clim. change* **9**, 374–378 (2019).
7. Selmi, R., Hammoudeh, S., Kasmaoui, K., Sousa, R. M. & Errami, Y. The dual shocks of the COVID-19 and the oil price collapse: a spark or a setback for the circular economy? *Energy Econ.* **109**, 105913 (2022).
8. Uekert, T. et al. Technical, economic, and environmental comparison of closed-loop recycling technologies for common plastics. *ACS Sustain. Chem. Eng.* **11**, 965–978 (2023).
9. WRAP. *Composition of plastic waste collected via kerbside*, <https://wrap.org.uk/resources/report/composition-plastic-waste-collected-kerbside> (2018).
10. Kim, Y. K. in *Polyolefin Fibres* 135–155 (Elsevier, 2017).
11. Ammala, A. et al. An overview of degradable and biodegradable polyolefins. *Prog. Polym. Sci.* **36**, 1015–1049 (2011).
12. Vasile, C. *Handbook of polyolefins*. (CRC press, 2000).
13. TA Instruments. *Understanding Rheology of Thermoplastic Polymers, 2023*, https://www.tainstruments.com/pdf/literature/AAN013_V_1_U_Thermoplast.pdf (2023).
14. Gijsman, P. & Fiorio, R. Long term thermo-oxidative degradation and stabilization of polypropylene (PP) and the implications for its recyclability. *Polym. Degrad. Stab.* **208**, 110260 (2023).
15. Cuadri, A. & Martin-Alfonso, J. The effect of thermal and thermo-oxidative degradation conditions on rheological, chemical and thermal properties of HDPE. *Polym. Degrad. Stab.* **141**, 11–18 (2017).
16. Gooneie, A. et al. Enhanced PET processing with organophosphorus additive: Flame retardant products with added-value for recycling. *Polym. Degrad. Stab.* **160**, 218–228 (2019).
17. Oblak, P., Gonzalez-Gutierrez, J., Zupančič, B., Aulova, A. & Emri, I. Processability and mechanical properties of extensively recycled high density polyethylene. *Polym. Degrad. Stab.* **114**, 133–145 (2015).
18. Smith, P. et al. A data-driven analysis of HDPE post-consumer recycle for sustainable bottle packaging. *Res. Conserv. Recycl.* **205**, 107538 (2024).
19. Bashirgonbadi, A. et al. Accurate determination of polyethylene (PE) and polypropylene (PP) content in polyolefin blends using machine learning-assisted differential scanning calorimetry (DSC) analysis. *Polym. Test.* **131**, 108353 (2024).
20. Boronat, T., Seguí, V., Peydro, M. & Reig, M. Influence of temperature and shear rate on the rheology and processability of reprocessed ABS in injection molding process. *J. Mater. Process. Technol.* **209**, 2735–2745 (2009).
21. Hamad, K., Kaseem, M. & Deri, F. Recycling of waste from polymer materials: An overview of the recent works. *Polym. Degrad. Stab.* **98**, 2801–2812 (2013).
22. Jung, H. et al. Review of polymer technologies for improving the recycling and upcycling efficiency of plastic waste. *Chemosphere* **320**, 138089 (2023).
23. Markandeya, N., Joshi, A. N., Chavan, N. N. & Kamble, S. P. Plastic recycling: challenges, opportunities, and future aspects. *Adv. Mater. Recycl. Waste*, 317–356 (2023).
24. Boldizar, A., Jansson, A., Gevert, T. & Möller, K. Simulated recycling of post-consumer high density polyethylene material. *Polym. Degrad. Stab.* **68**, 317–319 (2000).
25. Pitzer, L., Sandfort, F., Strieth-Kalthoff, F. & Glorius, F. Inter-molecular radical addition to carbonyls enabled by visible light photoredox initiated hole catalysis. *J. Am. Chem. Soc.* **139**, 13652–13655 (2017).
26. Mi, D. et al. Effects of phase morphology on mechanical properties: oriented/unoriented PP crystal combination with spherical/micro-fibrillar PET phase. *Polymers* **11**, 248 (2019).
27. Jakubowicz, I. Evaluation of degradability of biodegradable polyethylene (PE). *Polym. Degrad. Stab.* **80**, 39–43 (2003).
28. Samuel, C., Parpaite, T., Lacrampe, M.-F., Soulestin, J. & Lhost, O. Melt compatibility between polyolefins: Evaluation and reliability of interfacial/surface tensions obtained by various techniques. *Polym. Test.* **78**, 105995 (2019).
29. Vollmer, I. et al. Beyond mechanical recycling: giving new life to plastic waste. *Angew. Chem. Int. Ed.* **59**, 15402–15423 (2020).
30. Schyns, Z. O., Patel, A. D. & Shaver, M. P. Understanding poly(ethylene terephthalate) degradation using gas-mediated simulated recycling. *Resour. Conserv. Recycl.* **198**, 107170 (2023).
31. Angelopoulos, A. et al. Tackling faults in the industry 4.0 era—a survey of machine-learning solutions and key aspects. *Sensors* **20**, 109 (2019).
32. Law, K. L., Sobkowicz, M. J., Shaver, M. & Hahn, M. E. Untangling the chemical complexity of plastics to improve life cycle outcomes. *Nat. Rev. Mater.* **9**, 657–667 (2024).
33. Pinheiro, L. A., Chinelatto, M. A. & Canevarolo, S. V. The role of chain scission and chain branching in high density polyethylene during thermo-mechanical degradation. *Polym. Degrad. Stab.* **86**, 445–453 (2004).
34. Kealy, T. Rheological analysis of the degradation of HDPE during consecutive processing steps and for different processing conditions. *J. Appl. Polym. Sci.* **112**, 639–648 (2009).
35. García-Franco, C. A., Harrington, B. A. & Lohse, D. J. Effect of short-chain branching on the rheology of polyolefins. *Macromolecules* **39**, 2710–2717 (2006).
36. Aurrekoetxea, J., Sarrionandia, M., Urrutibeascoa, I. & Maspoch, M. L. Effects of recycling on the microstructure and the mechanical properties of isotactic polypropylene. *J. Mater. Sci.* **36**, 2607–2613 (2001).
37. da Costa, H. M., Ramos, V. D. & Rocha, M. C. Rheological properties of polypropylene during multiple extrusion. *Polym. Test.* **24**, 86–93 (2005).
38. Parada, G. A. & Zhao, X. Ideal reversible polymer networks. *Soft Matter* **14**, 5186–5196 (2018).
39. Münstedt, H. & Schwarzl, F. R. *Deformation and flow of polymeric materials*. (Springer, 2014).
40. Münstedt, H. Rheological measurements and structural analysis of polymeric materials. *Polymers* **13**, 1123 (2021).
41. Trinkle, S. & Friedrich, C. Van Gurp-Palmen-plot: a way to characterize polydispersity of linear polymers. *Rheol. Acta* **40**, 322–328 (2001).
42. Trinkle, S., Walter, P. & Friedrich, C. Van Gurp-Palmen plot II—classification of long chain branched polymers by their topology. *Rheol. Acta* **41**, 103–113 (2002).
43. Harlin, A. & Heino, E. L. Comparison of rheological properties of cross-linked and thermal-mechanically degraded HDPE. *J. Polym. Sci. Part B Polym. Phys.* **33**, 479–486 (1995).
44. Stadler, F. J. et al. Dependence of the zero shear-rate viscosity and the viscosity function of linear high-density polyethylenes on the mass-average molar mass and polydispersity. *Rheol. Acta* **45**, 755–764 (2006).

45. Locati, G., Pegoraro, M. & Nichetti, D. A model for the zero shear viscosity. *Polym. Eng. Sci.* **39**, 741–748 (1999).
46. Tung, L. Melt viscosity of polyethylene at zero shear. *J. Polym. Sci.* **46**, 409–422 (1960).
47. Kock, C., Aust, N., Grein, C. & Gahleitner, M. Polypropylene/polyethylene blends as models for high-impact propylene-ethylene copolymers, part 2: Relation between composition and mechanical performance. *J. Appl. Polym. Sci.* **130**, 287–296 (2013).
48. Kock, C., Gahleitner, M., Schausberger, A. & Ingolic, E. Polypropylene/polyethylene blends as models for high-impact propylene-ethylene copolymers, part 1: Interaction between rheology and morphology. *J. Appl. Polym. Sci.* **128**, 1484–1496 (2013).
49. Góra, M. et al. Surface-enhanced nucleation in immiscible polypropylene and polyethylene blends: The effect of polyethylene chain regularity. *Polymer* **282**, 126180 (2023).
50. Bashirgonbadi, A. et al. Accurate determination of polyethylene (PE) and polypropylene (PP) content in polyolefin blends using machine learning-assisted differential scanning calorimetry (DSC) analysis. *Polym. Test.* **131**, 108353 (2024).
51. Jordan, A. M. et al. Role of crystallization on polyolefin interfaces: an improved outlook for polyolefin blends. *Macromolecules* **51**, 2506–2516 (2018).

Acknowledgements

The Natural Environment Research Council is acknowledged for funding research (NE/V01045X/1, NE/V010549/1) (M.P.S.). The University of Manchester, the Engineering and Physical Sciences Research Council and Unilever are also acknowledged for funding as part of the EPSRC CAFE4DM Prosperity Partnership (EP/R00482X/1) (A.D.P., M.P.S.). This work used equipment based at the Henry Royce Institute for Advanced Materials (EPSRC grants EP/R00661X/1, EP/S019367/1, EP/P025021/1 and EP/P025498/1) (M.P.S.) and the Sustainable Materials Innovation Hub, funded through the European Regional Development fund (OC15R19P) (M.P.S.).

Author contributions

A.D.P., Z.O.G.S. and M.P.S. are responsible for conceptualising of the study. A.D.P. and T.W.F. performed experiments, with A.D.P. responsible for formal analysis of results, investigation, methodology development

and model development. A.D.P. produced the original manuscript with T.W.F., Z.O.G.S. and M.P.S. reviewing and editing. M.P.S. was responsible for supervision and funding acquisition.

Competing interests

The authors declare no competing interests.

Additional information

Supplementary information The online version contains supplementary material available at <https://doi.org/10.1038/s41467-024-52856-8>.

Correspondence and requests for materials should be addressed to Michael P. Shaver.

Peer review information *Nature Communications* thanks Krishnamurthy Jayaraman and Zdenek Stary for their contribution to the peer review of this work. A peer review file is available.

Reprints and permissions information is available at <http://www.nature.com/reprints>

Publisher's note Springer Nature remains neutral with regard to jurisdictional claims in published maps and institutional affiliations.

Open Access This article is licensed under a Creative Commons Attribution 4.0 International License, which permits use, sharing, adaptation, distribution and reproduction in any medium or format, as long as you give appropriate credit to the original author(s) and the source, provide a link to the Creative Commons licence, and indicate if changes were made. The images or other third party material in this article are included in the article's Creative Commons licence, unless indicated otherwise in a credit line to the material. If material is not included in the article's Creative Commons licence and your intended use is not permitted by statutory regulation or exceeds the permitted use, you will need to obtain permission directly from the copyright holder. To view a copy of this licence, visit <http://creativecommons.org/licenses/by/4.0/>.

© The Author(s) 2024